Optics Letters

Cavity enhanced parametric homodyne detection of a squeezed quantum comb

Yuhang Tian,[1] Xiaocong Sun,[1] Yajun Wang,[1,2,3] Qinghui Li,[1] Long Tian,[1,2] and Yaohui Zheng[1,2,4]

[1]*State Key Laboratory of Quantum Optics and Quantum Optics Devices, Institute of Opto-Electronics, Shanxi University, Taiyuan, Shanxi 030006, China*
[2]*Collaborative Innovation Center of Extreme Optics, Shanxi University, Taiyuan, Shanxi 030006, China*
[3]*e-mail: YJWangsxu@sxu.edu.cn*
[4]*e-mail: yhzheng@sxu.edu.cn*

Received 22 October 2021; revised 11 December 2021; accepted 19 December 2021; posted 20 December 2021; published 21 January 2022

A squeezed state with higher-order sidebands is a valuable quantum resource for channel multiplexing quantum communication. However, balanced homodyne detection used in nonclassical light detection has a trade-off performance between the detection bandwidth and clearance, in which the verification of a highly squeezing factor faces a challenge. Here, we construct two optical parametric amplifiers with cavity enhancement; one is for the generation of a −10.5 dB squeezed vacuum state, and the other is for all-optical phase-sensitive parametric homodyne detection. Finally, −6.5 dB squeezing at the carrier with 17 pairs of squeezing sidebands (bandwidth of 156 GHz) is directly and simultaneously observed. In particular, for the cavity-enhanced parametric oscillation and detection processes, we analyze the limiting factors of the detectable bandwidth and measurement deviation from the generated value, which indicates that the length difference and propagation loss between two optical parametric amplifiers should be as small as possible to improve the detection performance. The experimental results confirm our theoretical analysis.

https://doi.org/10.1364/OL.446645

Quantum noise in a quantized electromagnetic optical field or vacuum is responsible for physical effects such as the fluctuations of two quadratures, amplitude and phase, which implies a minimum uncertainty relation for those noncommuting observables. It sets the fundamental limits on the sensitivity or signal-to-noise ratio (SNR) of the measurement, i.e., for the applications of quantum precision measurement [1,2], quantum computation [3–5], and quantum communication [6–11]. Optical parametric amplifiers (OPAs) have been used to prepare squeezed states, wherein the fluctuation in one quadrature is increased and that of the other quadrature is reduced below the minimum uncertainty level [12–17], allowing for an improvement in the measurement sensitivity or SNR beyond the standard quantum limit (SQL). However, all applications require that we can verify the highly squeezing factor across the whole spectrum.

A squeezed state with bandwidth up to 2.5 THz has been recently reported via a single-pass waveguide OPA, but the electrical circuit's bandwidths of the detection and feed-forward control limit the detectable bandwidth to several gigahertz [18]. Therefore, a fully parallel optical homodyne detection was demonstrated via a single-pass all-optical phase-sensitive parametric process to break through the limitations of the electrical circuits for balanced homodyne detection (BHD). Ideally, the phase-sensitive parametric homodyne detection (PHD) can cover the bandwidth across the spectral acceptance bandwidth of the nonlinear medium, i.e., via spontaneous four-wave mixing (FWM) in a photonic crystal fiber (PCF) or OPA in a periodically poled $LiNbO_3$ (PPLN) waveguide [19–21]. However, the single-pass PHD that has low nonlinear interaction strength restricts the detection performance to a relatively low level.

An OPA with cavity enhanced nonlinear interaction has the capacity to produce the highest squeezing level up to 15 dB [12]. A squeezed quantum comb, covering several free spectral ranges (FSRs), has also been demonstrated [22–25], and the squeezing factor has been raised to the 10 dB level [26–28]. To compensate for the limited bandwidth of BHD, a pair of frequency-shifted bichromatic local oscillators (LOs) is prepared, exploiting acousto-optic modulators (AOMs) [29] or electro-optic modulators (EOMs) [26–28,30]. Thus, the upper limit of the detection bandwidth is transferred to the modulation capability, about tens of gigahertz. It is necessary to find a solution to all-optical PHD that is sufficient to evaluate a highly squeezing factor.

Here, we demonstrate an all-optical phase-sensitive PHD of a broadband squeezing quantum comb via a cavity-enhanced scheme. Owing to its sufficient nonlinear interaction strength, a quantum noise reduction of 6.5 dB is achieved for the first time. On account of the difference between cavity-enhanced and single-pass PHDs, we analyze the influence of the length difference and propagation loss between two OPAs on detection performance. Seventeen pairs of squeezing quantum combs from one OPA are directly observed with a bandwidth of 156 GHz by carefully optimizing the experimental parameter. The result beats the mark of the maximum squeezing degree measurement with an all-optical phase sensitive PHD.

In the parametric amplification process, one of the two quadratures of the injected beam can be set to the amplified status, whereas the other is attenuated to satisfy the uncertainty relation. As long as sufficient amplification is achieved, the output field primarily represents the information of the amplified quadrature without coupled additional noise [19,20]. The amplification bandwidth is limited only by the phase-matching condition of the nonlinear medium, which can easily span the spectral acceptance bandwidth of the squeezing measurement to several to 100 THz [19,20], for our case, it is 2 THz [Fig. 1(c), details of the models and discussion can be found in the third section of the supplementary materials in Ref. [26]]. This approach offers a quadrature selective quantum measurement for a broadband noise spectrum detection, namely PHD.

The squeezing measurement in PHD is uniform to BHD [19,20]. OPA1 is pumped by a second harmonic wave (2ν beam 1) to produce a squeezed vacuum state (beam 2), which presents as a frequency comb pattern [the block diagram in Fig. 1(a)] and acts as a seed field of OPA2. OPA2 works in a phase-sensitive amplifier status. The pump light (beam 3) of OPA2 plays the same role as the LO in BHD, i.e., providing a classical gain to amplify the squeezed or anti-squeezed quadrature. OPA2

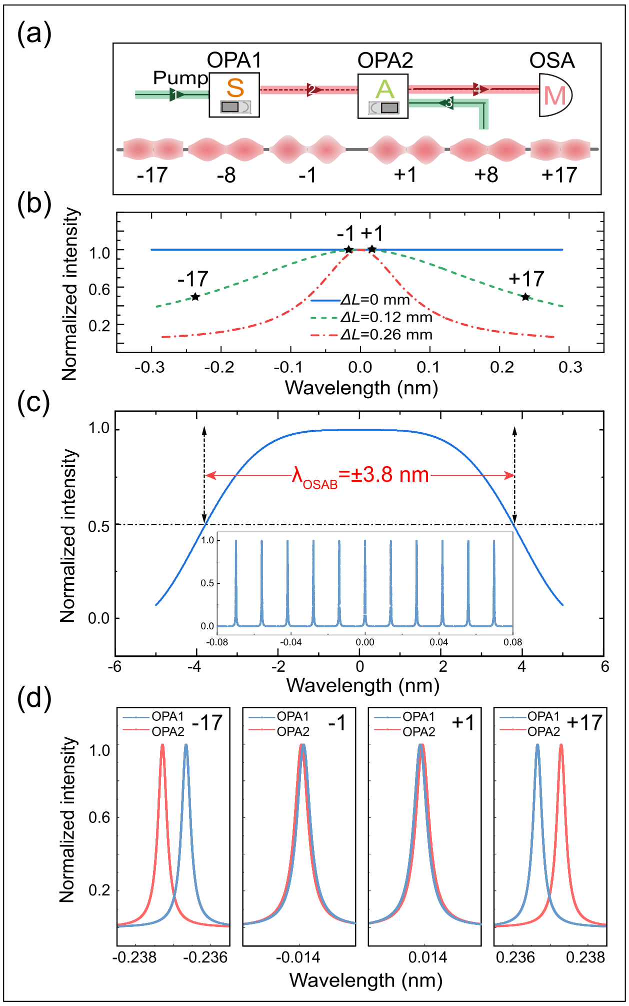

Fig. 1. (a) Schematic illustration and (b)–(d) theoretical demonstration of cavity enhanced output characters of the cascade OPAs of all-optical phase-sensitive configuration. (a) Schematic illustration for parametric homodyne detection (PHD). (b) Nonlinear interaction bandwidth reduction induced by length difference of the two OPAs. (c) Ideal nonlinear interaction bandwidth without length difference. (d) Cavity detuning of OPA2 versus OPA1. OPA, optical parametric amplifier.

transforms the variances of the input into an optical intensity signal (beam 4), which is measured with an optical spectrum analyzer (OSA). When normalizing the output to the intensity of an amplified vacuum (SQL) overflowing from OPA2, the squeezing R'_- or anti-squeezing R'_+ based on PHD is given by [19,20]: $R'_{-/+} = \frac{1}{1+G^2}R_{+/-} + \frac{G^2}{1+G^2}R_{-/+}$, where G is the gain factor. When OPA2 is seeded with a vacuum field, $R_- = R_+ = 1$, and corresponds to the SQL of the PHD. Here, $R_- = -10\log_{10} V_-$, $R_+ = -10\log_{10} V_+$ are the squeezing or anti-squeezing degree of the output field from OPA1, and $V_{-/+}$ is the squeezing or anti-squeezing noise variance. A higher gain G will result in a lower measurement error. Here, 16 dB of gain ($G = 40$) is enough to measure the squeezing level correctly.

Differing from the technology in Ref. [19,20], we analyze a pair of cascade OPAs with cavity enhancement for squeezed state generation and detection. Under this circumstance, the output of the OPA presents a frequency comb sideband spectrum of $\lambda_n = \lambda_0 + n * FSR$ [the illustration in Fig. 1(c)], where λ_0 is the wavelength of the carrier, n is the order and λ_n is nth-order sideband mode, $FSR = \frac{c}{2L_{1,2}}$ is the free spectral range of the cavity, c is the speed of light, $L_{1,2}$ is the resonance length, and ΔL is that of the length difference. Ideally, if the OPA's parameters are identical, the two frequency comb sidebands completely overlap with each other in the frequency domain. Then, OPA2 is fabricated to beat all the squeezing sidebands in the whole phase-matching bandwidth of OPA1, without attenuating the squeezing level, such as the blue solid line in Fig. 1(b). The normalized transmission intensity of the frequency comb sidebands can be expressed as [31]

$$t_{OPA} = \left| \frac{\sqrt{\left(1-r_1^2\right)\left(1-r_2^2\right)}\, e^{\frac{i\pi\Delta}{FSR}}}{1 - r_1 r_2 e^{\frac{2i\pi\Delta}{FSR}}} \right|^2, \quad \textbf{(1)}$$

where r_1, r_2 are the reflectivity of the two ends of the OPA cavity, and Δ is the wavelength's detuning relative to the carrier of the input field.

In practice, the two cavities have an inevitable difference in length (ΔL). If OPA2 is used as a PHD, its bandwidth will be limited by ΔL. In this case, the length distinction is equivalent to a frequency detuning $\Delta\nu$ for the OPA1's first-order sideband mode, and increases to $n\Delta\nu$ for the nth-order sideband. This phenomenon draws on a squeezing strength decrease owing to a weaker nonlinear interaction and lower coupling efficiency of the squeezing beam in OPA2, and becomes more serious with the increase of the sideband order. The results are shown with the green dash and red dash–dot lines in Figs. 1(b) and 1(d), which indicate that a larger ΔL induces a narrower bandwidth of the PHD. Considering the frequency detuning $\Delta\nu$ induced by ΔL, the measured squeezing and anti-squeezing variances of the nth sideband of the OPA1 can be modified as

$$V_{n,-/+} = 1 \mp \frac{4*\eta*\sqrt{p/p_{th}}}{\left(1 \pm \sqrt{p/p_{th}}\right)^2 + 4*\left(\frac{\lambda_f}{\Delta\lambda}\right)^2}, \quad \textbf{(2)}$$

where $\lambda_f = \lambda_{f_0} + n * \Delta\lambda_{FSR}$, $\eta = 1 - l$ is the detection efficiency of PHD technique, l is the total transmission loss of the measurement process, p is the pump power of OPA1, p_{th} is the threshold power of OPA1, $\Delta\lambda$ is the full width at half maximum (FWHM) of OPA1, λ_{f_0} is the analysis wavelength, and $\Delta\lambda_{FSR}$ is the difference of spectral regions between OPA1 and OPA2.

Figure 2 shows the schematic of our experimental setup, which is divided into two stations: squeezed vacuum generation

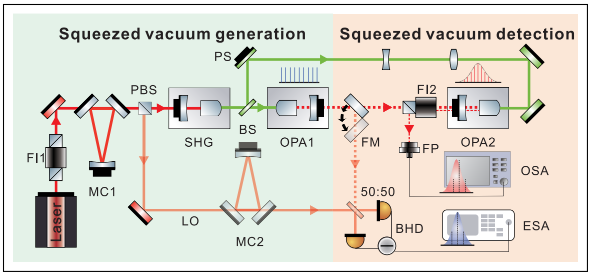

Fig. 2. Schematic of the experimental setup for squeezed vacuum generation and detection. FI, faraday isolator; MC1,2, mode cleaners; PBS, polarization beam splitter; SHG, second harmonic generator; BS, beam splitter; PS, phase shifter; OPA1,2, optical parametric amplifiers; FM, flip mirror; FP, fiber port; LO, local oscillator; 50:50, 50:50 beam splitter; BHD, balanced homodyne detector; OSA, optical spectrum analyzer; ESA, electrical spectrum analyzer.

and detection. We employ a continuous-wave (CW) single-frequency laser at 1064 nm as the laser source, most of which is for the second harmonic generator (SHG, 500 mW), the remaining part is for the LO. The harmonic wave is sequentially divided into two beams for OPAs pumping. Two mode cleaners (MCs) are used for classical quadrature noise and spatial fundamental mode purification. The OPAs are semi-monolithic cavities composed of a PPKTP crystal (10 mm × 2 mm × 1 mm) and a piezo actuated concave mirror [14,15]. The convex face of PPKTP ($R = 12$ mm) is coated with high reflectivity (HR) for 1064 nm and high transmission (HT) for 532 nm, which serves as one end mirror of the OPA. The plane front face of the crystal is coated with anti-reflectivity (AR) for both wavelengths. A concave mirror ($R = 30$ mm) has a transmissivity of 18% for 1064 nm and HR for 532 nm, and the reverse side is AR coated, serving as the output coupler.

In squeezed vacuum detection, two homodyne technologies are established to record the squeezing levels output from OPA1. Therein, BHD with a quantum efficiency higher than 99% is fabricated for squeezing degree calibration of the carrier [14,15]. OPA2 works in a phase-sensitive amplifier status with incorporating an OSA to fulfill a PHD process. The squeezed vacuum state exporting from OPA1 passes through the Faraday isolator (FI2), and enters into OPA2 to transfer the squeezing signal into a classical intensity one. Then the amplified signal is reflected by OPA2, and coupled into an optical fiber guiding to an OSA (Yokogawa, AQ6370D) that has a wavelength scanning range of 600–1700 nm. The weighted intensity distribution for each frequency is distinguished by measuring the intensity of the optical field by scanning the OSA. Therefore, the broadband detection bandwidth property still survives at the completion of the detection process. A flip mirror (FM) between OPA1 and FI2 is inserted to switch the measurement between BHD and PHD. A phase shifter (PS) in the pump field is implemented to switch the measurement between squeezing and anti-squeezing quadratures in the PHD process. The detailed parameters of the experiment data are listed in Table 1.

First, a −10.5 dB (12 dB) squeezed (anti-squeezed) vacuum state of the carrier is directly observed with BHD at a pump power of 200 mW and an analysis frequency of 3 MHz. Subsequently, OPA2 working on resonance with the carrier frequency of OPA1 is pumped with a harmonic power of 300 mW ($G = 44$) before squeezing injection. Limited by SHG power, this is a best compromise for sufficient gain of the OPA2. We expect to achieve a higher squeezing level with enough power. The amplified vacuum field is calibrated to be the SQL of PHD. Then, squeezing enters into the OPA2 to perform a phase-sensitive amplifier measurement. The amplified signal is coupled into an OSA to record 17 pairs of squeezing sidebands in a wavelength range of 1064.15–1064.75 nm (bandwidth of 156 GHz). The results are shown in Fig. 3. The data points represent the squeezing and anti-squeezing level of the frequency sidebands, and the adjacent data points are divided by the FSR of OPA1. All the measurement results are normalized to SQL, and fitted with Eq. (2) and the parameters in Table 1. The fitted results are in good agreement with the experimental results in a spectrum range of 156 GHz. The maximum squeezing (anti-squeezing) level is measured to be −6.5 dB (9.3 dB) at the carrier frequency, and reduced to −1.2 dB (1.4 dB) at the 17th one. Meanwhile, the pump power dependence of squeezing and anti-squeezing for the carrier are measured at the analysis frequency of 3 MHz, and the results are matched very well by the fitted results with [32]: $R_{-/+} = l + (1 - l)\, e^{\mp 2\sqrt{a \times p}}$, where $a = 6.0\ \mathrm{W}^{-1}$ is the nonlinear conversion efficiency of the OPA1. The total transmission loss l is determined to be 12.5% [Fig. 4(a)]. All the data in Figs. 3 and 4(a) are recorded by scanning the pump field's phase of OPA2 with a phase shifter. One scanning curve of the carrier's squeezing variance is provided as an example in Fig. 4(b), which corresponds to the data in the red and blue shaded areas of Figs. 3 and 4(a). Here, we omit the similar results of the other sidebands to avoid repetition.

The experimental and theoretical results both demonstrate that the length difference between the OPAs is responsible for the detectable bandwidth limitation and squeezing declension of the cavity enhanced PHD technique. The fitting results in Fig. 3 also provide a methodology for precise measurement of the length difference ΔL between the two OPAs, which can be translated into a frequency detuning for all-optical phase-sensitive measurement. The detuning accumulates with the increasing of

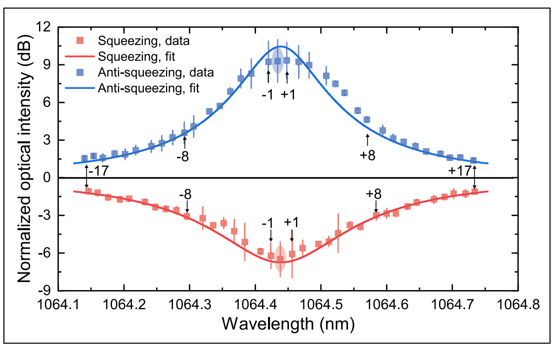

Fig. 3. Squeezing measurement for 17 pairs of sidebands with PHD method. Upper curve, squeezing; lower curve, anti-squeezing.

Table 1. Experimental Parameters in the Calculations of Figs. 3 and 4

Cavity	r_1 (%)	r_2(%)	L (mm)	FSR (GHz)	p_{th} (mW)	λ_0 (nm)	$\Delta\lambda_{FSR}$ (nm)	$\Delta\lambda$ (nm)	λ_{f_0} (nm)
*OPA*1(2)	99.9	82	36.8(36.72)	3.326(3.332)	410	1064.446	2.30×10^{-5}	4.04×10^{-4}	1.15×10^{-5}

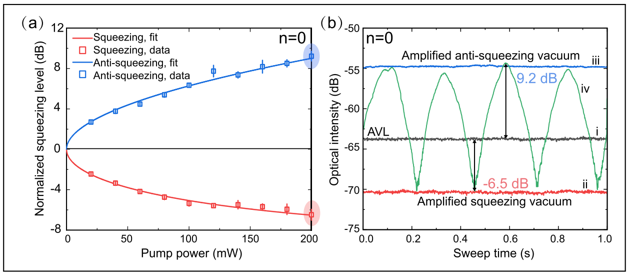

Fig. 4. (a) Noise power of squeezing (upper curve) and anti-squeezing (lower curve) as a function of pump power of OPA1. (b) Optical intensity as a function of sweep time. Trace i is the amplified vacuum level (AVL). Traces ii and iii are amplified squeezed and anti-squeezed vacuum state, respectively. Trace iv is the amplified squeezed vacuum with relative phase between squeezed vacuum from OPA1 and the pump beam of OPA2 is swept.

sideband order, and hence a squeezing level decay is observed in the optical spectrum. Additionally, the maximum detectable squeezing is confined to a lower level of −6.5 dB, which arises from the transmission loss l between OPA1 and OPA2, which mainly comes from the imperfect transmission of FI2 (2.5%) and squeezing beam mode mismatching to OPA2 (10%). The low mode matching efficiency roots from a serious undercoupled character of OPA1. Only a weak signal can be used to inject into OPA2, which makes it very difficult to achieve a perfect mode matching. Furthermore, the maximum wavelength accuracy (±0.01 nm) and resolution (0.02 nm) of the OSA are also limiting factors for the maximum squeezing degree, owing to a frequency difference between the sidebands and the OSA. The system loss before OSA can be reduced by improving the propagation loss in FI2 and mode-matching efficiency of OPA2. More careful cavity length calibration will prompt the measured bandwidth approach to the phase-matching bandwidth of the PPKTP.

We have experimentally demonstrated an all-optical phase-sensitive detection of a squeezing quantum comb via cavity-enhanced phase-sensitive PHD. According to the theoretical analysis, we found that the length difference and propagation loss between two OPAs is the main limitation affecting the detection bandwidth and measurement deviation. By optimizing these experimental parameters, 17 pairs of squeezed sidebands are directly observed with a maximum noise reduction of −6.5 dB. We expect that higher-order sideband modes can be uniformly evaluated, exploiting the innovative technique for cavity length calibration.

Funding. National Natural Science Foundation of China (62027821, 11654002, 11874250, 12174234, 62035015); National Key Research and Development Program of China (2020YFC2200402); Key Research and Development Projects of Shanxi Province (201903D111001); Program for Sanjin Scholar of Shanxi Province.

Disclosures. The authors declare no conflicts of interest.

Data Availability. Data underlying the results presented in this paper are not publicly available at this time but may be obtained from the authors upon reasonable request.

REFERENCES

1. H. Vahlbruch, D. Wilken, M. Mehmet, and B. Willke, Phys. Rev. Lett. **121**, 173601 (2018).
2. B.-B. Li, J. Bílek, U. B. Hoff, L. S. Madsen, S. Forstner, V. Prakash, C. Schäfermeier, T. Gehring, W. P. Bowen, and U. L. Andersen, Optica **5**, 850 (2018).
3. N. C. Menicucci, Phys. Rev. Lett. **112**, 120504 (2014).
4. J.-I. Yoshikawa, Y. Miwa, A. Huck, U. L. Andersen, P. van Loock, and A. Furusawa, Phys. Rev. Lett. **101**, 250501 (2008).
5. X. Su, S. Hao, X. Deng, L. Ma, M. Wang, X. Jia, C. Xie, and K. Peng, Nat. Commun. **4**, 2828 (2013).
6. L. S. Madsen, V. C. Usenko, M. Lassen, R. Filip, and U. L. Andersen, Nat. Commun. **3**, 1083 (2012).
7. A. Furusawa, J. L. Sorensen, S. L. Braunstein, C. A. Fuchs, H. J. Kimble, and E. S. Polzik, Science **282**, 706 (1998).
8. Q. Wang, Y. Wang, X. Sun, Y. Tian, W. Li, L. Tian, X. Yu, J. Zhang, and Y. Zheng, Opt. Lett. **46**, 1844 (2021).
9. S. Liu, Y. Lou, and J. Jing, Nat. Commun. **11**, 3875 (2020).
10. N. Huo, Y. Liu, J. Li, L. Cui, X. Chen, R. Palivela, T. Xie, X. Li, and Z. Y. Ou, Phys. Rev. Lett. **124**, 213603 (2020).
11. Y. Liu, N. Huo, J. Li, and X. Li, Opt. Lett. **43**, 5559 (2018).
12. H. Vahlbruch, M. Mehmet, K. Danzmann, and R. Schnabel, Phys. Rev. Lett. **117**, 110801 (2016).
13. H. Vahlbruch, M. Mehmet, S. Chelkowski, B. Hage, A. Franzen, N. Lastzka, S. Goßler, K. Danzmann, and R. Schnabel, Phys. Rev. Lett. **100**, 033602 (2008).
14. W. Yang, S. Shi, Y. Wang, W. Ma, Y. Zheng, and K. Peng, Opt. Lett. **42**, 4553 (2017).
15. S. Shi, Y. Wang, W. Yang, Y. Zheng, and K. Peng, Opt. Lett. **43**, 5411 (2018).
16. J. Arnbak, C. S. Jacobsen, R. B. Andrade, X. Guo, J. S. Neergaard-Nielsen, U. L. Andersen, and T. Gehring, Opt. Express **27**, 37877 (2019).
17. T. Eberle, V. Händchen, and R. Schnabel, Opt. Express **21**, 11546 (2013).
18. T. Kashiwazaki, N. Takanashi, T. Yamashima, T. Kazama, K. Enbutsu, R. Kasahara, T. Umeki, and A. Furusawa, APL Photonics **5**, 036104 (2020).
19. Y. Shaked, Y. Michael, R. Z. Vered, L. Bello, M. Rosenbluh, and A. Pe'er, Nat. Commun. **9**, 609 (2018).
20. N. Takanashi, A. Inoue, T. Kashiwazaki, T. Kazama, K. Enbutsu, R. Kasahara, T. Umeki, and A. Furusawa, Opt. Express **28**, 34916 (2020).
21. J. Li, Y. Liu, N. Huo, L. Cui, S. Feng, X. Li, and Z. Y. Ou, Phys. Rev. A **101**, 053801 (2020).
22. J. Roslund, R. M. de Araújo, S. Jiang, C. Fabre, and N. Treps, Nat. Photonics **8**, 109 (2014).
23. T. Serikawa, J.-I. Yoshikawa, S. Takeda, H. Yonezawa, T. C. Ralph, E. H. Huntington, and A. Furusawa, Phys. Rev. Lett. **121**, 143602 (2018).
24. Z. Yang, M. Jahanbozorgi, D. Jeong, S. Sun, O. Pfister, H. Lee, and X. Yi, Nat. Commun. **12**, 4781 (2021).
25. R. Senior, G. Milford, J. Janousek, A. Dunlop, K. Wagner, H.-A. Bachor, T. Ralph, E. Huntington, and C. Harb, Opt. Express **15**, 5310 (2007).
26. S. Shi, L. Tian, Y. Wang, Y. Zheng, C. Xie, and K. Peng, Phys. Rev. Lett. **125**, 070502 (2020).
27. S. Shi, Y. Wang, L. Tian, J. Wang, X. Sun, and Y. Zheng, Opt. Lett. **45**, 2419 (2020).
28. L. Tian, S. Shi, Y. Li, Y. Wu, W. Li, Y. Wang, Q. Liu, and Y. Zheng, Opt. Lett. **46**, 3989 (2021).
29. W. Li, X. Yu, and J. Zhang, Opt. Lett. **40**, 5299 (2015).
30. M. Pysher, Y. Miwa, R. Shahrokhshahi, R. Bloomer, and O. Pfister, Phys. Rev. Lett. **107**, 030505 (2011).
31. A. S. Villar, Am. J. Phys. **76**, 922 (2008).
32. T. Hirano, K. Kotani, T. Ishibashi, S. Okude, and T. Kuwamoto, Opt. Lett. **30**, 1722 (2005).